PERKIN 2

Palladium-catalysed oxidation of alcohols to carbonyl compounds with 1,2-dichloroethane as the primary oxidant: a theoretical study †

Gadi Rothenberg,*[a] Stéphane Humbel *[b] and Jacques Muzart [b]

[a] *York Green Chemistry Group, Chemistry Department, University of York, Heslington, York, UK YO10 5DD. E-mail: gr8@york.ac.uk*
[b] *Unité Mixte de Recherche 6519 "Réactions Sélectives et Applications", CNRS–Université de Reims Champagne-Ardennes, B.P. 1039, 51687 REIMS Cedex 2, France. E-mail: stephane.humbel@univ-reims.fr*

Received (in Cambridge, UK) 9th March 2001, Accepted 24th July 2001
First published as an Advance Article on the web 12th September 2001

Homogeneous palladium chloride catalyses the oxidation of alcohols to aldehydes or ketones in 1,2-dichloroethane (DCE). The active catalytic species is regenerated by the dechlorination of DCE to ethylene. This catalytic cycle is studied here using non-local density functional theory. The insertions of "naked" Pd, of HPdCl, and of $PdCl_2$ into the C–Cl bond of DCE are examined in detail, and it is shown that the most likely inserting species is Pd, then HPdCl and $PdCl_2$. Two distinct reaction pathways are proposed and investigated, namely insertion of HPdCl into the C–Cl bond, followed by HCl abstraction, and abstraction of HCl from HPdCl, followed by oxidative insertion of a "naked" Pd atom into the C–Cl bond. Both paths converge on the same species but the former is found to involve lower energies. Entropy effects, ligand effects and possible mechanisms for the formation of ethylene in this system are discussed. Based on these results, the complete oxidation cycle from methanol to formaldehyde is calculated as a model reaction for the dehydrogenation of alcohols in this system. It is shown that the original catalytic species does not necessarily need to be regenerated to complete a the catalytic cycle. Ligand effects and entropy effects are considered. The choice of methanol as a model of alcohol is discussed.

Introduction

Dichloromethane (DCM) and 1,2-dichloroethane (DCE) are common industrial chemicals.[1] As organic solvents their advantages are undisputed,[2] but their effects on the environment are causing concern.[3] In this context, it is worthwhile to investigate alternatives for their use.

One interesting option is the application of DCE as an oxidant. Previously, one of us has described the oxidation of alcohols using sodium carbonate and catalytic quantities of both $PdCl_2$ and Adogen 464 in refluxing DCE.[4,5] It was shown that (*i*) DCE was the regenerator of the active palladium species, with concurrent formation of ethylene (Scheme 1) and (*ii*) that the main role of the ammonium salt was to solubilise the palladium salt, as $[PdCl_2][(\text{Adogen } 464)_2]$.[6,7] The overall process (Scheme 1) is meritorious, as it equates to a one-pot oxidation and aliphatic dechlorination, with the advantage that a new carbon–carbon bond is also formed. Since our preliminary report, others have also used DCE to regenerate Pd(II).[8,9]

In the literature, the oxidation of (*R*-BINAP)Pd(0) into (*R*-BINAP)$PdCl_2$ by DCE,[10] the reaction of the C–Cl bond of DCE with the unsaturated $Pd(PPh_3)$ complex,[11] and the elimination[12] of ethylene from (dppe)$PdCl(CH_2CH_2Cl)$ have been studied. The light-induced formation of $(dpm)_2Pd_2Cl_2$ [a Pd(I) complex] and ethylene from $(dpm)_3Pd_2$ and DCE has also been reported.[13] These reports led us to envisage that under our oxidation conditions the regeneration of the active catalyst could be due to a reaction of the transient species HPdCl with DCE, rather than to an oxidative insertion of Pd(0) species into a C–Cl bond of DCE as was previously suggested.[4] Furthermore, in the oxidation of allylic alcohols we obtained a mixture of saturated and α,β-unsaturated carbonyl compounds, where the formation of the former may be attributed to a 1,2-addition–elimination sequence between palladium hydride and the C=C double bond.[14]

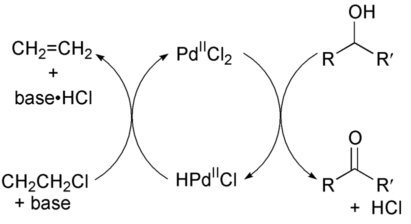

Scheme 1

$$HPdCl + ClCH_2CH_2Cl \longrightarrow PdCl_2 + CH_2{=}CH_2 + HCl \quad (1)$$

It is difficult to set up experiments to differentiate between the various catalytic pathways in this complex oxidation–dechlorination system. However, the fundamentals of the dechlorination and oxidation reactions may be elucidated through computational studies. Here, we report the results of a detailed density functional theory (DFT) study on the mechanism of the regeneration of $PdCl_2$ from HPdCl and DCE [eqn. (1)], and compare the feasibility of oxidative insertion and HCl elimination processes in this system. Using methanol as a model alcohol, we studied the completion of the catalytic cycle to give ethylene, formaldehyde and $PdCl_2$.

Computational methods

Calculations were performed on Compaq and SGI computers using the three-parameter Becke–Lee–Yang–Parr hybrid

---

† Electronic supplementary information (ESI) available: Tables of absolute energies and structural parameters for all of the computed species. See http://www.rsc.org/suppdata/p2/b1/b102256n/

DOI: 10.1039/b102256n

(B3LYP) density functional method.[15–17] The basis set we used was based on the LANL2DZ "basis set",[18] which combined either a relativistic effective core potential (RECP) plus a double-ζ Gaussian basis (for chlorine and palladium) after Hay and Wadt, or simply an all electron double-ζ Gaussian basis (for carbon and hydrogen) after Dunning and Hay.[19] The following polarization functions were added to the LANL2DZ description: for the geometry optimization (henceforth this basis will be referred to as BS_I) we added one set of d orbitals for the carbon, the oxygen, and the chlorine atoms [exponent values, $d_C = 0.8$, $d_O = 0.8$ and $d_{Cl} = 0.75$, respectively, were taken from the standard 6-31G(d) basis set]. For the energy calculations, BS_I was extended to include the palladium atom with an additional set of f orbitals (*i.e.*, $BS_{II} = BS_I + f_{Pd}$) using an exponent value[20] of $f_{Pd} = 1.472$.

We used the Gaussian 98 suite of programs throughout this study.[21] All calculations were performed using the default parameters of this program (5D and 7F orbitals for "general" basis sets). However, a tight criterion was applied for the SCF density threshold (10^{-8}). All the optimized structures were obtained with small residual forces, and characterized as minima or transition states using the analytical second-derivative analysis at the same level (B3LYP/BS_I).

The following theoretical treatment does not include the R_4N^+ or Cl^- ions but focuses on the Pd reactivity. In solution, each palladium atom is likely to be co-ordinated to four ligands and any abstraction or insertion process would be counterbalanced by ligand (*e.g.* Cl^- or R_4N^+) co-ordination. In the case of HCl abstraction, the loss of a ligand in the medium would be counterbalanced by the HCl. Roughly speaking, all molecules in the condensed phase interact together and can be considered as a unique system.[22] The total entropy of the system would thus remain essentially unchanged, and so we approximate $\Delta G \approx \Delta H$. This approximation may be void when a gas is produced that can "escape" from the reaction medium (*e.g.* when an ethylene molecule is formed, *vide infra*). For that case, we considered the process as a single system that dissociates into two parts, with an entropy change that we estimated at 30 entropy units (a value that is often encountered for gas-phase dissociations). At rt, this would lead to a $T\Delta S$ contribution of *ca.* 10 kcal mol^{-1}.

In the following discussions we used only the Zero Point energy Corrected (ZPC) ΔH values calculated at the highest level that was available to us (B3LYP/BS_{II}//B3LYP//BS_I). The ZPC has been calculated at the optimization level (B3LYP//BS_I). Note that in all of the following energy calculations the contribution of the f orbitals was minor or negligible.

Results and discussion

In constructing a model system for the regeneration of the active Pd(II) species from HPdCl and DCE [eqn. (1) above] we envisaged two distinct pathways: (a) insertion of HPdCl into the C–Cl bond, followed by HCl abstraction (Scheme 2, left); and (b) abstraction of HCl from HPdCl, followed by oxidative insertion of the Pd atom into the C–Cl bond (Scheme 2, right). These two paths converge when HCl is released in path (a). The main difference between the two paths is that the abstraction of HCl can occur either before or after the Pd insertion into the C–Cl bond of DCE. We began by investigating various Pd oxidative insertions, depending on the nature of the Pd species: HPdCl as in pathway (a), and a "naked" Pd atom as in (b). For comparison, we also examined the reactivity of the regenerated catalyst Pd(II)Cl_2 *vis-à-vis* DCE.

Palladium insertion reactions

The oxidative insertion of a "naked" palladium atom into the C–Cl bond of CH_3Cl has been investigated in detail by Bickelhaupt *et al.* using a local density approach.[23] Fig. 1 shows the geometrical differences obtained after reoptimizing the oxidative transition state reported in that study using non-local density functionals. While we noted quite a few differences (*e.g.* systematically longer bond distances using the B3LYP approximation), the structures qualitatively agree, especially with regard to the small Pd–H distance and the corresponding elongated C–H bond. Both indicate an agostic Pd–H interaction during the insertion. As non-local density functionals are reputedly better than their local counterparts[24] we shall refer in the following only to the B3LYP level.

Table 1 Relative energies for palladium insertions[a]

	ΔZPC_{BSI}[b]	ΔH_{BSI}[b]	ΔH_{BSII}[b]	ΔH_{BSII}[c]
Pd(0) insertion				
1	0.2	−8.8	−9.0	0.0
2	−1.4	4.3	4.0	13.0
3	−0.8	−25.8	−26.9	−17.9
HPdCl insertion				
4	0.8	−15.8	−15.8	0.0
5	−0.3	9.5	9.5	25.3
6	0.7	−11.1	−11.3	4.5
$PdCl_2$ insertion				
7	0.8	−15.5	−15.5	0.0
8	−0.7	15.4	15.5	31.0
9	0.0	0.3	0.3	15.8

[a] In kcal mol^{-1}, ZPC included. [b] Relative to the starting materials {catalyst (Pd(0), HPdCl or $PdCl_2$) + DCE}. [c] Relative to the associated complex (**1**, **4**, **7**).

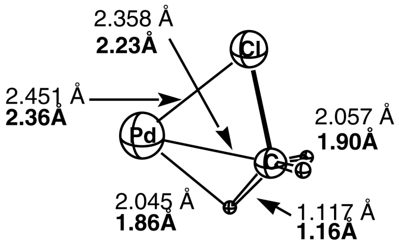

Fig. 1 Geometrical parameters for the insertion of a "naked" Pd into a C–Cl bond at two levels of calculation: local density from ref. 22 (bold) and B3LYP/BSI.

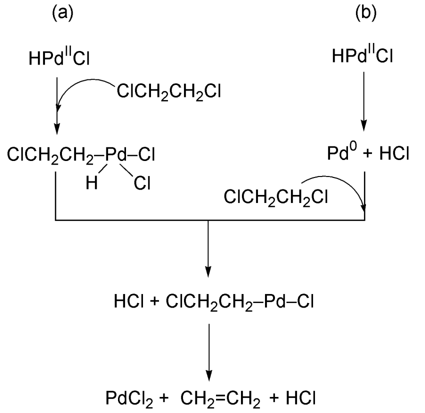

Scheme 2

Key geometrical and energy values for the reactants (compounds **1**, **4** and **7**), transition structures (compounds **2**, **5** and **8**) and products (compounds **3**, **6** and **9**) for the three respective insertion reactions are shown in Fig. 2 and in Table 1.[25] In agreement with the previous study, we found that the palladium atom approaches the chloroalkane from the direction of the chlorine atom. Thus, an {R–Cl···Pd} and not a {Pd···R–Cl}

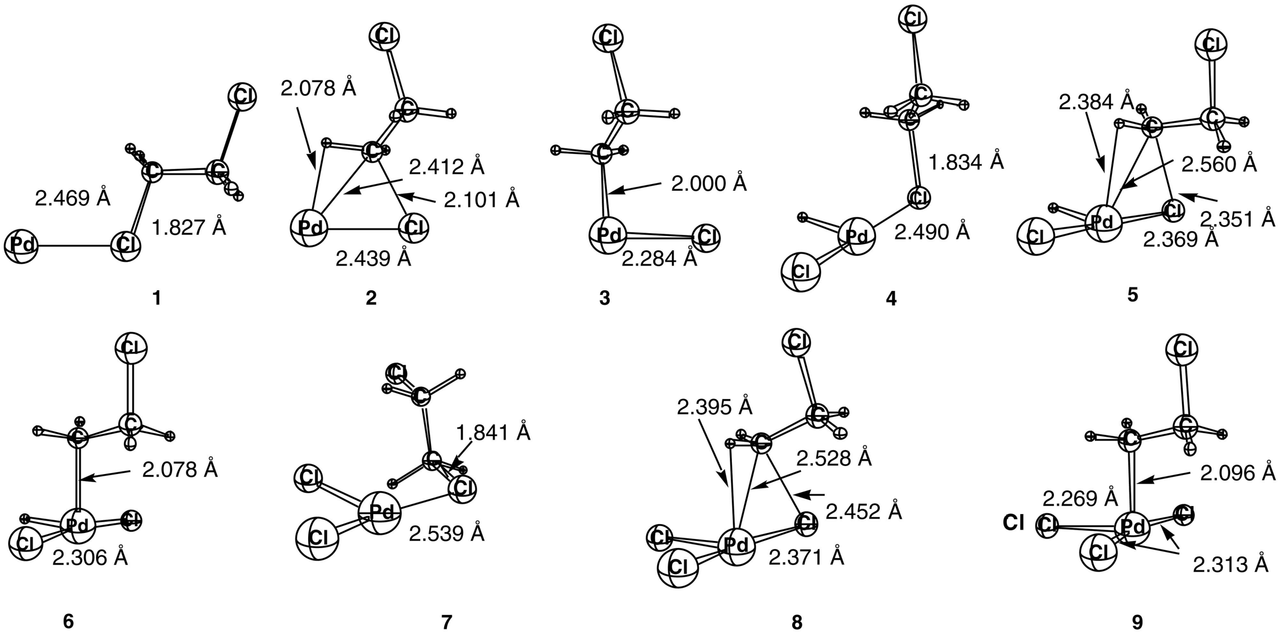

Fig. 2 Key geometrical parameters for the oxidative insertion of the "naked" Pd atom (**1**–**3**), HPdCl (**4**–**6**) and $PdCl_2$ (**7**–**9**) into the C–Cl of 1,2-dichloroethane as optimized at the B3LYP/BS_I level.

reactant complex is formed (the latter has been suggested as a precursor for an S_N2 type insertion process).[23] Moreover, the oxidative insertions were found to proceed *via* triangular, covalently bonded transition structures, rather than follow a dissociative pathway that would involve charge separation or free-radical species. It is significant that these similarities hold for both the "naked" palladium atom (*i.e.* reflect the *intrinsic reactivity* of palladium) as well as for the HPdCl and $PdCl_2$ molecules.

While there are geometrical similarities between the three activated complexes **2**, **5** and **8** that represent the transition structures, the agostic Pd–H interaction in the case of the "naked" Pd (structure **2**, $d_{Pd-H} = 2.08$ Å) is much reduced in the HPdCl and $PdCl_2$ transition states (structures **5** and **8**, respectively, $d_{Pd-H} = 2.39$ Å). The C–Cl activated bond in the TS also differs, which may indicate an early transition state in the case of **2** ($d_{C-Cl} = 2.10$ Å), and a late transition state in the case of **5** ($d_{C-Cl} = 2.35$ Å) and **8** ($d_{C-Cl} = 2.45$ Å). However, the absolute determination of which TS is earlier is difficult, as the Pd–C bond lengths make **2** later than **5** and **8**.

As indicated by the relative energies in Table 1, the Pd insertion is easier for the "naked" Pd(0) atom than for the Pd(II) species HPdCl and $PdCl_2$. For the transition structures, the value of the activation barrier[26] increased from the "naked" Pd (13.0 kcal mol^{-1}) to the substituted systems (25.3 kcal mol^{-1} for HPdCl and 31.0 kcal mol^{-1} for $PdCl_2$, respectively). This suggests that the insertion of the $PdCl_2$ is less likely. The same was evidenced for the insertion products, *viz.* an endothermic process (15.8 kcal mol^{-1}) for $PdCl_2$ *vs.* −17.9 kcal mol^{-1} for the insertion of the "naked" Pd atom.

Comparison between pathways (a) and (b)

Here, one has to take into account the palladium insertion *and* the abstraction of HCl, prior to the convergence of both pathways to structure **3**. Key structural parameters and energies of the potential energy surfaces for (a) and (b) are shown in Figs. 2 and 3 and in Table 2, and the energy profiles (ΔH) along pathways (a) and (b) are drawn in Fig. 4. The insertion of the palladium into the C–Cl bond is an important barrier in both cases. In pathway (a), the stable reactant complex **4** is formed, which then undergoes oxidative insertion of the Pd atom into the C–Cl bond (*vide supra*). Conversely, on pathway (b), the HCl abstraction from HPdCl and subsequent DCE coordination to the "naked" Pd leads to the structure {**1** + HCl}, which is 8.3 kcal mol^{-1} above the reactants. The aforementioned barrier of 13 kcal mol^{-1} for the insertion of the Pd

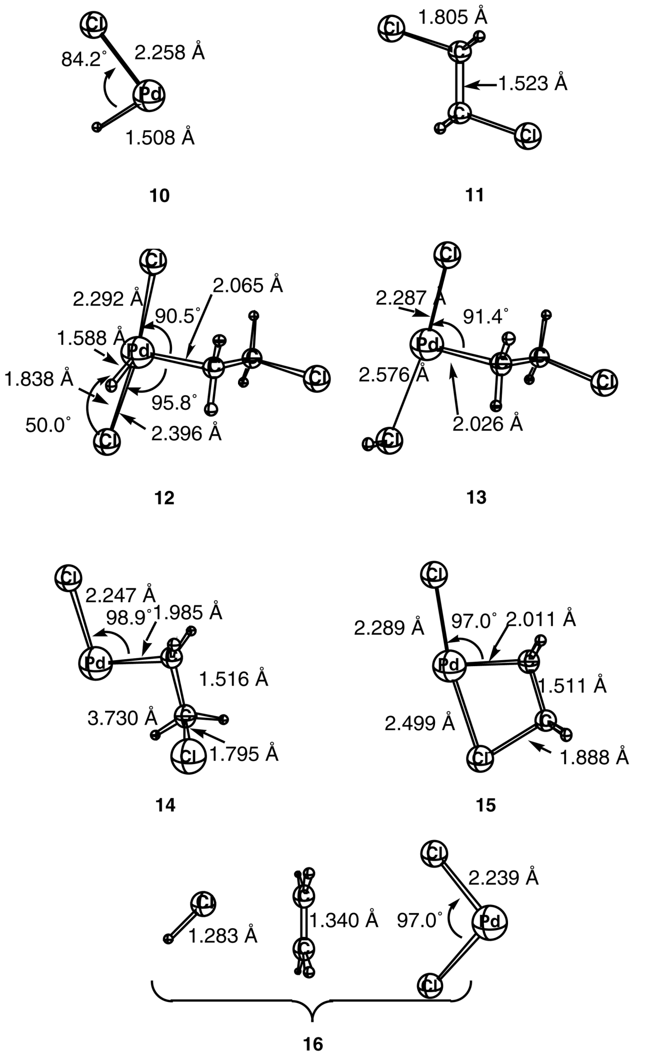

Fig. 3 Key geometrical parameters for the additional structures in pathways (a) and (b) as optimized at the B3LYP/BS_I level.

Table 2 Paths (*a*) and (*b*) for the alcohol oxidation[a]

	ΔZPC_{BSI}	ΔH_{BSI}	ΔH_{BSII}
Pathway (a)			
10 + DCE	0.0	0.0	0.0
4	0.8	−15.8	−15.8
5	−0.3	9.5	9.5
6	0.7	−11.1	−11.3
12	−0.6	−7.5	−7.7
13	0.5	−19.3	−19.3
Pathway (b)			
10 + DCE	0.0	0.0	0.0
Pd + HCl + DCE	−0.2	16.2	17.3
1 + HCl	0.0	7.3	8.3
2 + HCl	−1.6	20.4	21.2
Ethylene abstraction			
3 + HCl	−1.0	−9.6	−9.6
14 + HCl	−1.7	−8.3	−8.4
15 + HCl	−1.0	−18.8	−18.9
16	−3.8	9.7	9.5

[a] Energies relative to the starting materials {**10** + DCE} in kcal mol^{-1}, ZPC included.

atom into the C–Cl bond is added to this energy and renders the transition state **2** 21.2 kcal mol^{-1} higher than the reactants.

The large energy barrier for the transformation **4** ⟶ **5** ⟶ **6** may give the impression that (b) should be the favoured pathway, but since the actual starting points of both (a) and (b) would be lower due to the co-ordination of ligands, we suggest that pathway (a) is preferred as it involves inherently lower energies.

Ethylene formation

Following the convergence of (a) and (b) to structure **3**, we computed the energy changes for the dissociation of **3** into ethylene and $PdCl_2$, as evidenced by the experimental data.[4] We found that this reaction proceeds *via* the intermediate **15**, which features a four-membered heterocyclic ring. This intermediate conforms well with the computational parameters, and it is also easy to envisage its dissociation into the final reaction product **16**.

However, it is likely that the initial approximation of disregarding ligand effects in this system does not hold in this case. In the absence of ligands, the reaction pathway has to go through **15**, which is stabilized by the addition of the second chloride to the palladium atom in the formation of the four-membered ring. Conversely, in the actual solution, structure **3** is already stabilized by two chloride ions, so that the chlorine atom that is not attached to the palladium could leave through an intermolecular reaction with an ammonium cation R_4N^+ (see Scheme 3).[27] The overall reaction would be the formation of ethylene and the "pristine" catalyst $\{PdCl_2(R_4NCl)_2\}$ which could begin a new catalytic cycle with an incoming alcohol molecule.

Another mechanism is proposed in Scheme 4 where a ligand exchange occurs between a halide chloride and an alcohol molecule R_2CHOH. Through this exchange one obtains a new reactant complex for the alcohol oxidation, without actually regenerating the starting catalyst $[PdCl_2(NR_4Cl)_2]$. In this case, the formation of ethylene would occur during the alcohol oxidation.

Completion of the catalytic cycle

Here we considered the overall process of the catalytic oxidation of alcohols to carbonyl compounds. We chose the oxidation of methanol to formaldehyde as a model reaction in order to simplify the system. The results are summarized in Fig. 5. The corresponding structures **17**–**29** and their energy parameters are presented in Fig. 6 and Table 3.[25]

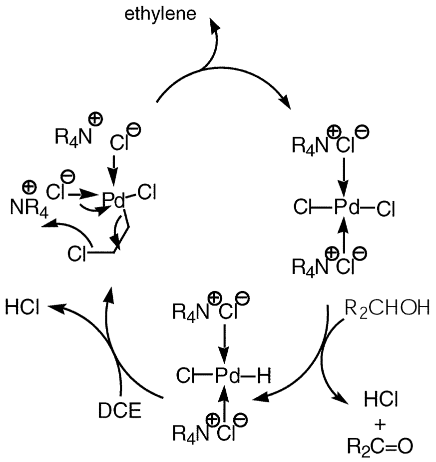

Scheme 3 Suggested pathway for $PdCl_2$ regeneration in the oxidation of alcohols (ligands included).

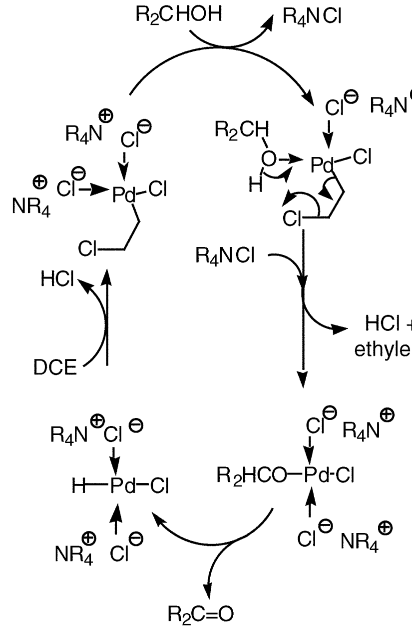

Scheme 4 Suggested pathway for alcohol oxidation (ligands included) that does not require the regeneration of the starting catalyst $\{PdCl_2(NR_4Cl)_2\}$.

The reaction sequence described in Scheme 3 is represented by the broken line in Fig. 5. Starting from structure **3**, $PdCl_2$ is formed *via* a mechanism involving NR_4Cl ligands (not computed). Following the formation of the associative reactant complex **17**, the activation of the alcohol O–H bond and the formation of the H–Cl bond involve structures which are about 40 kcal mol^{-1} higher in energy than the reactants. The HCl molecule can then be released for the last step of the oxidation (depicted in the rectangle in Fig. 5).

In the second path (shown in Scheme 4 and represented by a continuous bold line in Fig. 5), the activation of the alcohol O–H bond and the formation of the H–Cl bond involve structures which are at most *ca.* 26 kcal mol^{-1} higher than the reactants. Ethylene is finally released as well as HCl for the last step of the oxidation.

Before discussing the last part of the catalytic cycle, a brief comment on the entropy effects that should be associated with each part of the energy curves is in order. Since in the final part of the cycle ethylene escapes as a gas from the reaction mixture (*cf.* ref. 4) the corresponding ΔH values should be corrected for entropy changes. As discussed above, we used the value of 10

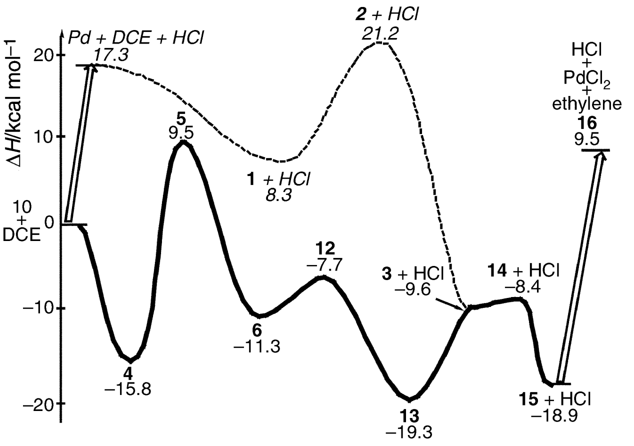

Fig. 4 Reaction energy profiles showing pathways (a) (continuous bold line and roman text) and (b) (broken line and italicized text). The arrows from {**10** + DCE} to {Pd + DCE + HCl} and from **15** to **16** represent reaction paths for which the intermediates and transition states could not be computed within our approximations.

Table 3 Paths for the alcohol oxidation as described in Schemes 3 (**17**–**24**) and 4 (**25**–**29**)[a]

	ΔZPC_{BSI}	ΔH_{BSI}	ΔH_{BSII}
17 + HCl + ethylene	−1.9	−16.3	−16.7
18 + HCl + ethylene	−6.8	42.0	41.2
19 + HCl + ethylene	−6.5	36.8	36.0
20 + HCl + ethylene	−7.2	36.5	35.6
21 + HCl + ethylene	−6.5	8.4	7.6
22 + 2HCl + ethylene	−6.7	20.2	19.6
23 + 2HCl + ethylene	−8.1	25.3	24.9
24 + 2HCl + ethylene	−9.9	9.0	8.7
25 + HCl	1.1	−31.9	−32.0
26 + HCl	−3.1	13.8	13.4
27 + HCl	−2.1	7.8	7.2
28 + HCl	−5.3	26.7	26.3
29 + HCl	−3.2	−18.7	−19.2
10 + 2HCl + ethylene + $H_2C{=}O$	−11.9	26.0	26.0

[a] Energies are in kcal mol^{-1}, relative to the starting materials {**10** + DCE + CH_3OH}, ZPC included. These values can be compared directly with those in Table 2.

kcal mol^{-1} as an approximation for $T\Delta S$ for an rt dissociation. This correction should apply to all the structures of the first path of the methanol oxidation. It would lower by 10 kcal mol^{-1} the whole broken-line curve and the last step in Fig. 5. Though the difference between the two mechanisms becomes smaller, the bold-line pathway is still favoured, its highest transition barrier being at *ca.* 26 kcal mol^{-1} (**28**) *vs.* *ca.* 31 kcal mol^{-1} (**18**).

The very last part of the alcohol oxidation (depicted in the rectangle in Fig. 5) involves a small barrier followed by the dissociation of **24** to the products HPdCl + $H_2C{=}O$ that are 26.0 kcal mol^{-1} above the reactants. This is of course the overall ΔH for the reaction R–OH + DCE ⟶ R=O + ethylene + 2HCl. However, even after correcting for the entropy contribution, the energetic cost is unsatisfactory for the continuation of the catalytic cycle. This result, *which does not depend on the proposed mechanism*, suggests that larger entropy effects may control the reaction, and/or that methanol may not be a good model candidate. We briefly investigated the latter hypothesis by calculating ΔH° for the oxidation of propan-2-ol to acetone, and found a much lower value (ΔH° = 14.4 kcal mol^{-1}).[25] With the correction of $T\Delta S$ the energy cost for propan-2-ol oxidation becomes only *ca.* 4 kcal mol^{-1}. However, while the choice of the alcohol significantly affects the overall ΔH° for the oxidation, it is not expected to modify much the whole catalytic mechanism, as the formaldehyde is released only in the last step.

Conclusions

Palladium insertion into the C–Cl bond is a key transformation in the catalytic oxidation of alcohols by DCE. Based on the energy differences for the insertion of the "naked" Pd atom,

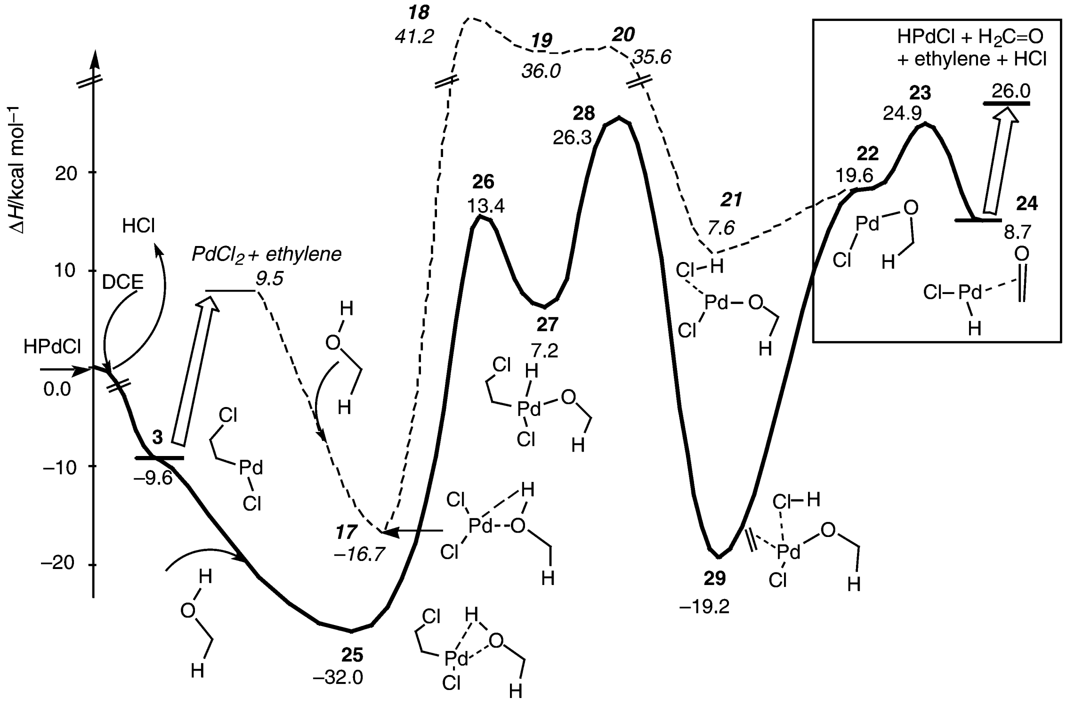

Fig. 5 Reaction energy profiles for the oxidation of MeOH with $PdCl_2$ (broken line, italicized text) and {**3**} (continuous line, roman text). The energies are given in kcal mol^{-1}, relative to the starting materials in Fig. 4, and corrected for the release of HCl and the inclusion of methanol. On going from HPdCl to **3**, a DCE molecule has come in and an HCl molecule has left. The arrows from **3** to {$PdCl_2$ + ethylene} and from **24** to {HPdCl + $H_2C{=}O$} represent reaction paths for which the intermediates and transition states could not be computed within our approximations. Note that the ordinate is discontinuous in the case of structures **18**, **19** and **20**.

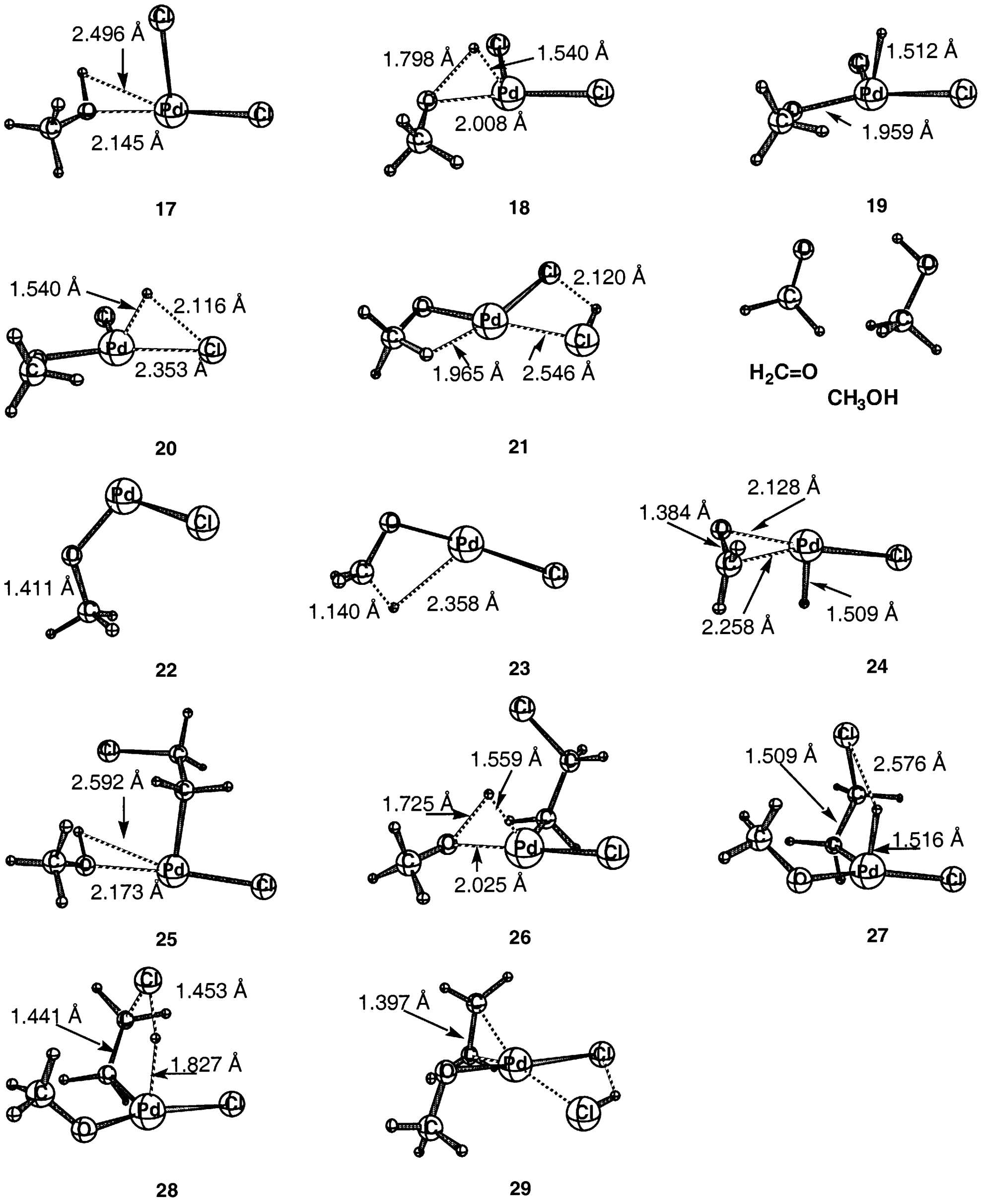

Fig. 6 Key geometrical parameters for the structures computed for the two paths of the alcohol oxidation as described in Schemes 3 (**17**–**24**) and 4 (**25**–**29**).

HPdCl and $PdCl_2$, we suggest that the reaction of the last two is less likely. The formation of ethylene is also an important step in the cycle due to its high energy barrier. Significantly, it is possible to start a new alcohol oxidation cycle using the intermediate structure **3**, so that regeneration of the starting catalyst ($PdCl_2$) is not a prerequisite.

Acknowledgements

We thank Dr C. Verma and Dr M. Reinhold (The University of York) for instructive discussions, the referees of this manuscript for insightful comments, the European Commission for a Marie Curie individual research fellowship (to G.R.), and *CRIHAN–Plan Interrégional du Bassin Parisien–Pôle interrégional de modélisation en sciences pour l'ingénieur, project 2001003*, for substantial allocation of computing time. Part of this work was carried out in the framework of the COST D12/0028/99 program.

References

1 *Cf.* current bulk prices (\$ kg^{-1}): DCM 0.88; DCE 0.37: *Chem. Market Rep.*, 2000, June 12, 257.
2 J. H. Atherton, in *Chemistry of Waste Minimisation*, ed. J. H. Clark, Blackie, Glasgow, 1995, pp. 417–440.
3 (*a*) J. H. Clark, *Green Chem.*, 2000, **2**, G35; J. H. Clark, *Green Chem.*, 2000, **2**, G39; (*b*) ENDS report No. 303, Environmental Data Services, London, April 2000, pp. 42–43; (*c*) for a comprehensive recent review discussing the environmental effects of chlorine-containing compounds, see N. Winterton, *Green Chem.*, 2000, **2**, 173.
4 S. Aït-Mohand, F. Hénin and J. Muzart, *Tetrahedron Lett.,*, 1995, **36**, 2473.
5 (*a*) S. Aït-Mohand and J. Muzart, *J. Mol. Catal. A: Chem.*, 1998, **129**, 135; (*b*) S. Aït-Mohand, F. Hénin and J. Muzart, *Organometallics*, 2001, **20**, 1683.
6 S. Bouquillon, A. du Moulinet d'Hardemare, M.-Th. Averbuch-Pouchot, F. Hénin and J. Muzart, *Polyhedron*, 1999, **18**, 3511.
7 Adogen 464 is a registered trademark of Ashland Chemical Co. for methyltrialkyl(C_8–C_{10})ammonium chloride.
8 S.-K. Kang, E.-Y. Namkoong and T. Yamaguchi, *Synth. Commun.*, 1997, **27**, 641.
9 A. N. Vedernikov, M. D. Sayakhov and B. N. Solomonov, *Mendeleev Commun.*, 1997, 205.
10 K. Ohrai, K. Kondo, M. Sodeoka and M. Shibasaki, *J. Am. Chem. Soc.*, 1994, **116**, 11737.
11 V. V. Grushin, *Organometallics*, 2000, **19**, 1888.
12 R. McCrindle, G. Ferguson, A. J. McAlees, G. J. Arsenault, A. Gupta and M. C. Jennings, *Organometallics*, 1995, **14**, 2741.
13 T. Tsubomura, A. Itsuki, M. Homma and K. Sakai, *Chem. Lett.*, 1994, 661.

14 R. F. Heck, *Palladium Reagents in Organic Synthesis*, Academic Press, London, 1985, pp. 19–20.

15 (*a*) A. D. Becke, *Phys. Rev. A*, 1988, **38**, 3098; (*b*) A. D. Becke, *J. Chem. Phys.*, 1993, **98**, 1372; (*c*) A. D. Becke, *J. Chem. Phys.*, 1988, **98**, 5648.

16 C. Lee, W. Yang and R. G. Parr, *Phys. Rev. B*, 1988, **37**, 785.

17 W. Koch and M. C. Holthausen, *A Chemist's Guide to Density Functional Theory*, Wiley–VCH, Weinheim, 2000.

18 P. J. Hay and W. R. Wadt, *J. Chem. Phys.*, 1985, **82**, 299.

19 T. H. Dunning, Jr. and P. J. Hay, in *Modern Theoretical Chemistry*, ed. H. F. Schaefer III, Plenum Press, New York, 1976, pp. 1–28.

20 A. W. Ehlers, M. Böhme, S. Dapprich, A. Gobbi, A. Höllwarth, V. Jonas, K. F. Köhler, R. Stegmann, A. Veldkamp and G. Frenking, *Chem. Phys. Lett.*, 1993, **208**, 111.

21 Gaussian 98, Revision A.7, M. J. Frisch, G. W. Trucks, H. B. Schlegel, G. E. Scuseria, M. A. Robb, J. R. Cheeseman, V. G. Zakrzewski, J. A. Montgomery, Jr., R. E. Stratmann, J. C. Burant, S. Dapprich, J. M. Millam, A. D. Daniels, K. N. Kudin, M. C. Strain, O. Farkas, J. Tomasi, V. Barone, M. Cossi, R. Cammi, B. Mennucci, C. Pomelli, C. Adamo, S. Clifford, J. Ochterski, G. A. Petersson, P. Y. Ayala, Q. Cui, K. Morokuma, D. K. Malick, A. D. Rabuck, K. Raghavachari, J. B. Foresman, J. Cioslowski, J. V. Ortiz, A. G. Baboul, B. B. Stefanov, G. Liu, A. Liashenko, P. Piskorz, I. Komaromi, R. Gomperts, R. L. Martin, D. J. Fox, T. Keith, M. A. Al-Laham, C. Y. Peng, A. Nanayakkara, C. Gonzalez, M. Challacombe, P. M. W. Gill, B. Johnson, W. Chen, M. W. Wong, J. L. Andres, C. Gonzalez, M. Head-Gordon, E. S. Replogle and J. A. Pople, Gaussian, Inc., Pittsburgh, PA, 1998.

22 For another approach to this problem, see Y.-D. Wu, K. W. K. Chan and Z. Xue, *J. Am. Chem. Soc.*, 1995, **117**, 9259.

23 F. M. Bickelhaupt, T. Ziegler and P. v. R. Schleyer, *Organometallics*, 1995, **14**, 2288.

24 For a discussion, see W. Koch and R. H. Hertwig, in *Encyclopedia of Computational Chemistry*, ed. P. v. R. Schleyer, Wiley, Chichester, 1998, vol. 1, pp. 689–700. See also ref. 17.

25 The absolute energies and other computational parameters for all the structures described here are available as part of the supporting information.

26 As calculated by the energy difference between the transition structures (**2**, **5** and **8**) and the reactant complexes (**1**, **4** and **7**), respectively.

27 Adding additional Cl^- ions as ligands results in di-anion species that are difficult to compute due to diffuse electrons.